Recent progress on drift-tearing analysis and verification

Jacob King, Scott Kruger
Tech-X Corporation

NIMROD Team Meeting Summer 2014

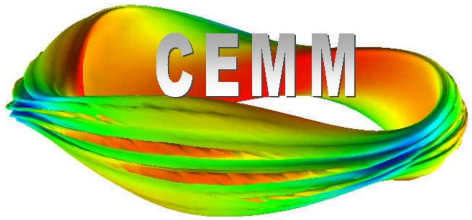

A manuscript is posted on arxiv, a subset of which has been submitted to PoP.

- See http://arxiv.org/abs/1407.3864

- This talk will focus on new developments over the last year:
  - Discussion of the experimentally relevant parameter space
  - New solution in PR2
  - Benchmarking
  - Eigenfunction plots

We want to characterize the fusion-plasma relevance of our new drift-tearing solutions.

- Although our initial motivation was to investigate drift-tearing for code verification, a relevance analysis is a response to controversies in the literature.
- Our new solutions for PR2, PR3 and PR4 use the NIMROD FLR model without ion gyroviscosity.

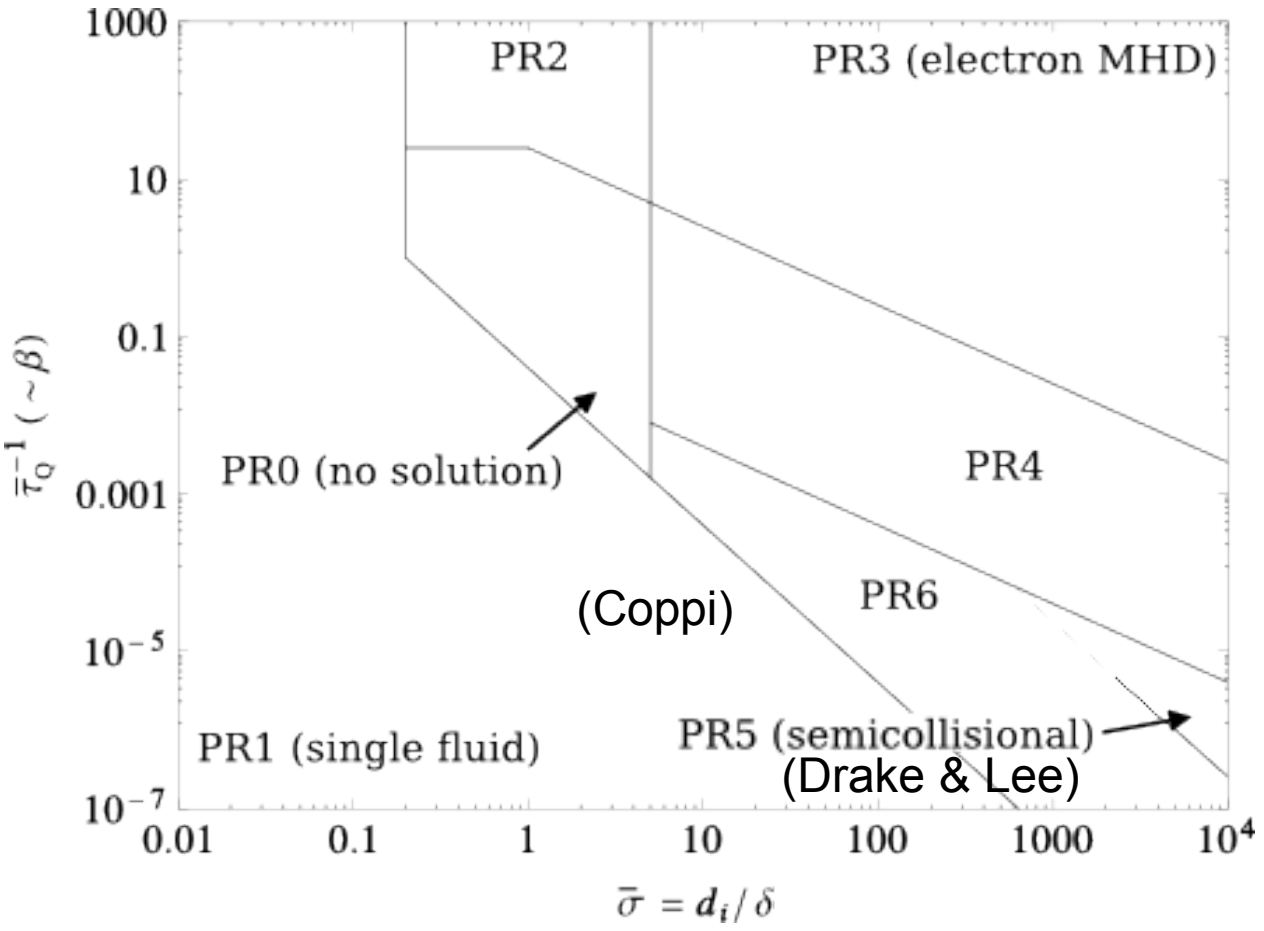

We use scan the following parameters to compute the location in parameter space for each potential case.

- Parameter range is chosen to approximate an experimental range.
- Each case uses the proper regime growth rate to compute the normalized parameter.

parameter	range
S	10^7-10^9
$k_\perp d_i$	0.01-1.0
β	0.005-0.1
$k_\perp^{-1}\Delta'$	0.5-20
ϵ_B	0.02-0.5

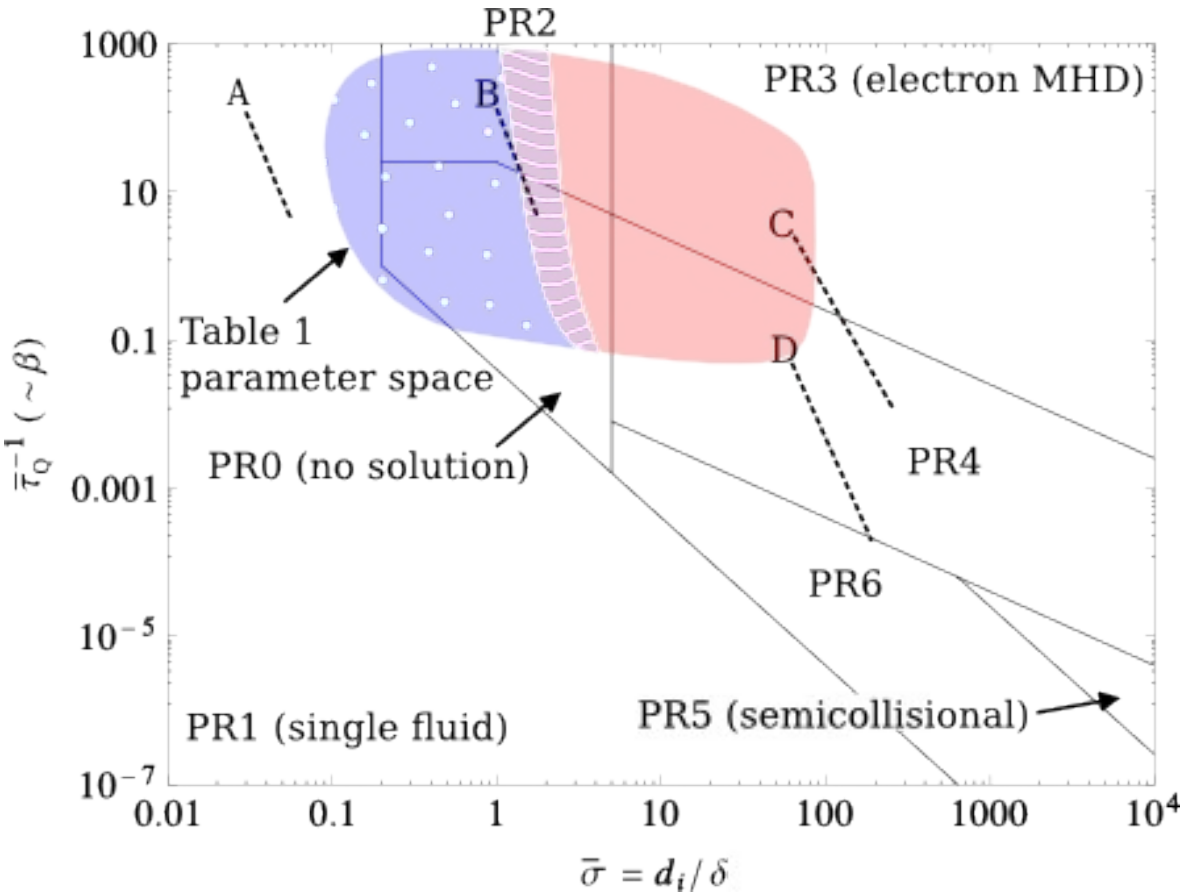

FLR parameter relative to the ion gyroradius reveals the regime of validity.

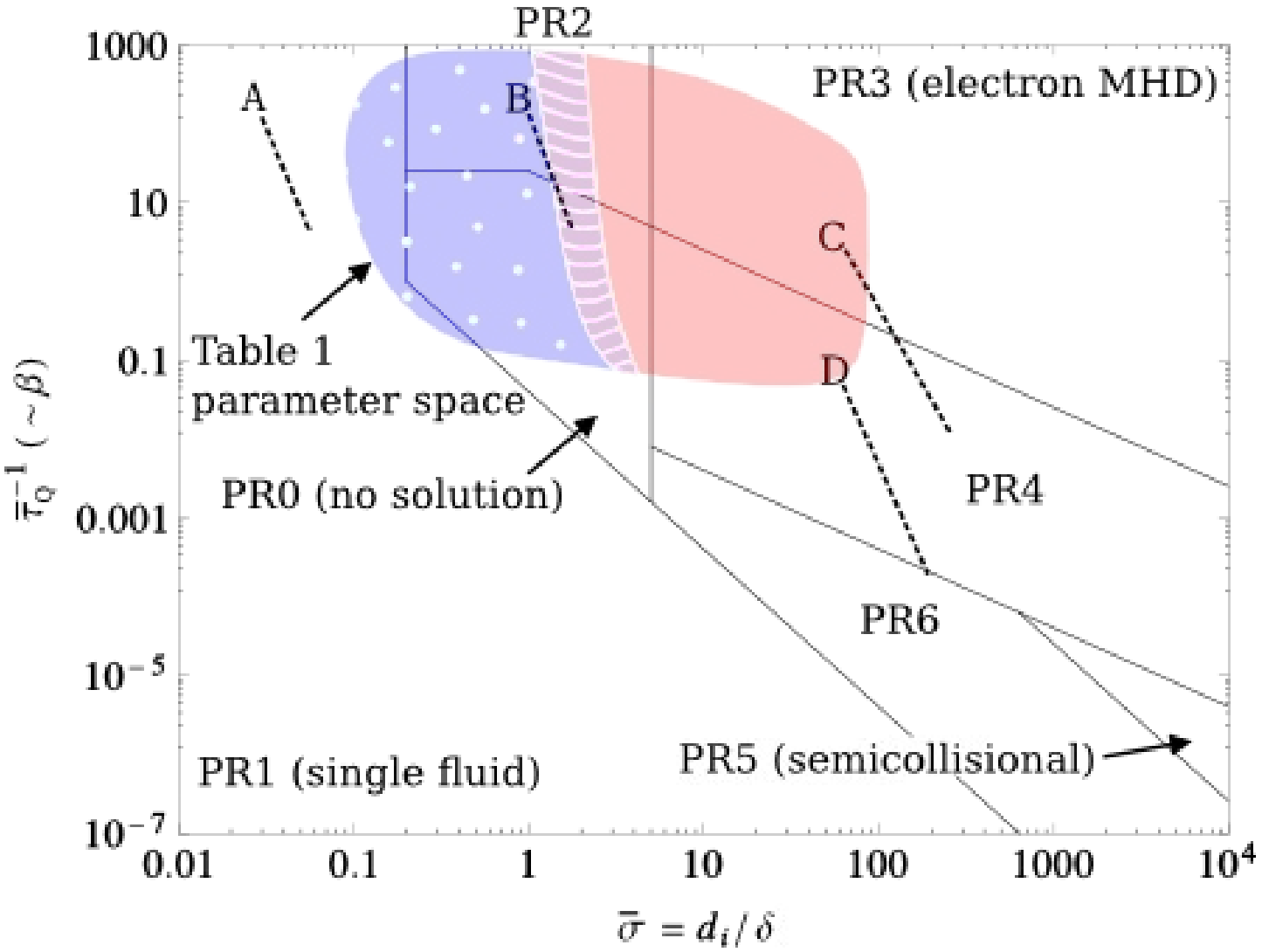

Not a 1-to-1 mapping between the normalized and unnormalized variables.

First-order FLR model is valid in blue region and invalid in red region. Purple region is mixed validity.

Validity chosen when ratio of ion gyroradius over layer width is less than a ¼.

New drift-tearing solution in PR2 is derived.

- Solution method uses transformation method of Ahedo and Ramos [NF 2009], but includes new (R, Λ) and modified (σ) terms.
- Details are in manuscript.

$$D = \int_{-\infty}^{\infty} d\bar{x}\left(1 - \bar{x}\bar{\xi} - \bar{x}\bar{Q}\right) = \frac{k_{\|}'\ \ \Delta'}{\hat{\gamma}_e \hat{\gamma}_{E\times B}^{1/4} S_g^{3/4}}$$

$$\bar{R} = \frac{\hat{\gamma}_{gvi}}{\hat{\gamma}_{E\times B}}\ , \quad \bar{\Lambda} = \frac{i\hat{\omega}_*}{\hat{\gamma}_e}\frac{\hat{\gamma}_{E\times B}}{\hat{\gamma}_{gvi}}$$

$$D = \sqrt{2}\Gamma\left(3/4\right)^2 f_2\left(\bar{\sigma}, \bar{R}, \bar{\Lambda}\right)$$

$$f_2\left(\bar{\sigma}, \bar{R}, \bar{\Lambda}\right) = \sum_{i=1,2} \frac{1}{2}\left[1 - \frac{\bar{\Lambda}\bar{R}}{2}\left((-1)^i\sqrt{1 + \frac{4}{\bar{R}\bar{\sigma}^2}} - 1\right)\right]\left[1 + (-1)^i\left(1 + \frac{4}{\bar{R}\bar{\sigma}^2}\right)^{-1/2}\right]$$

$$\times\left[\bar{R}^{-1} + \frac{\bar{\sigma}^2}{2} + (-1)^i\,\bar{\sigma}\sqrt{\frac{\bar{\sigma}^2}{4} + \bar{R}^{-1}}\right]^{-1/4}$$

Drift-frequency verification scans compare NIMROD with new analytics.

- As drift frequency is increase, cases move within beta-ion-skin-depth parameter space.
- Scans begin at A, B, C and D and progress along dashed lines as drift frequency is increased.

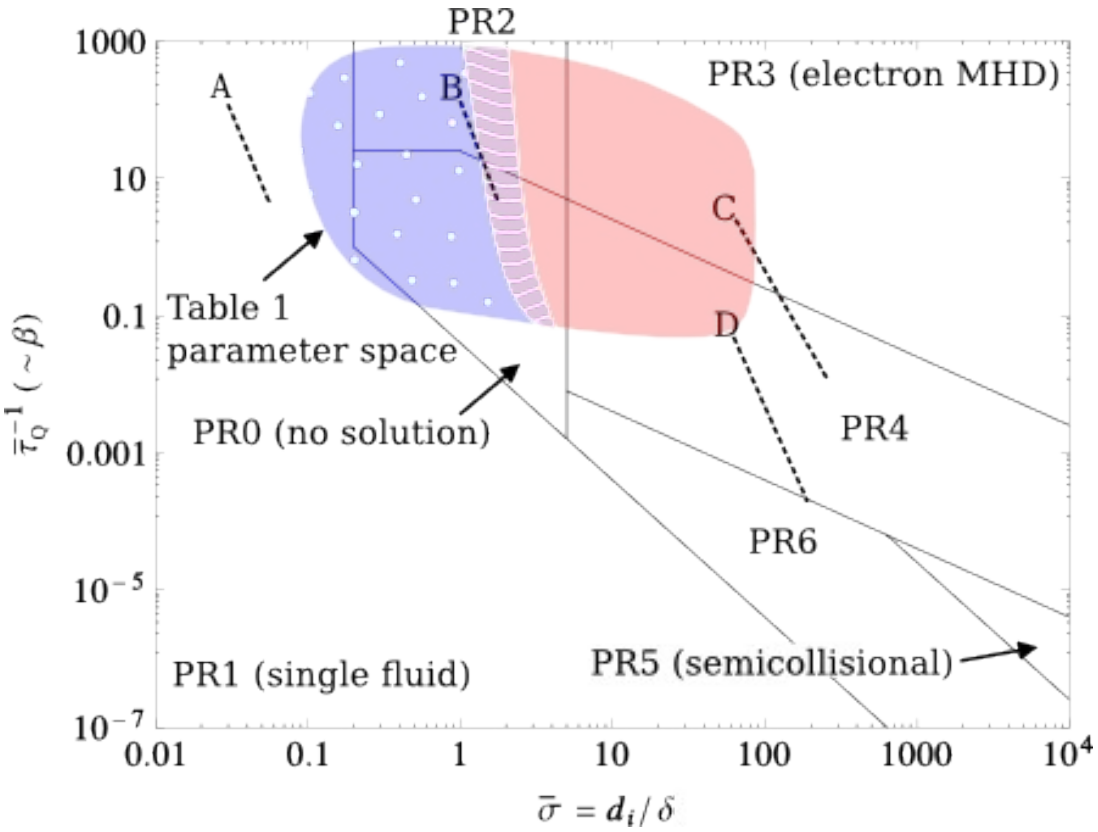

Our drift-frequency verification scans compare NIMROD with the new analytics.

- As the drift frequency is increase, cases move within the beta-ion-skin-depth parameter space.
- Scans begin at A, B, C and D and progress along the dashed lines as the drift frequency is increased.

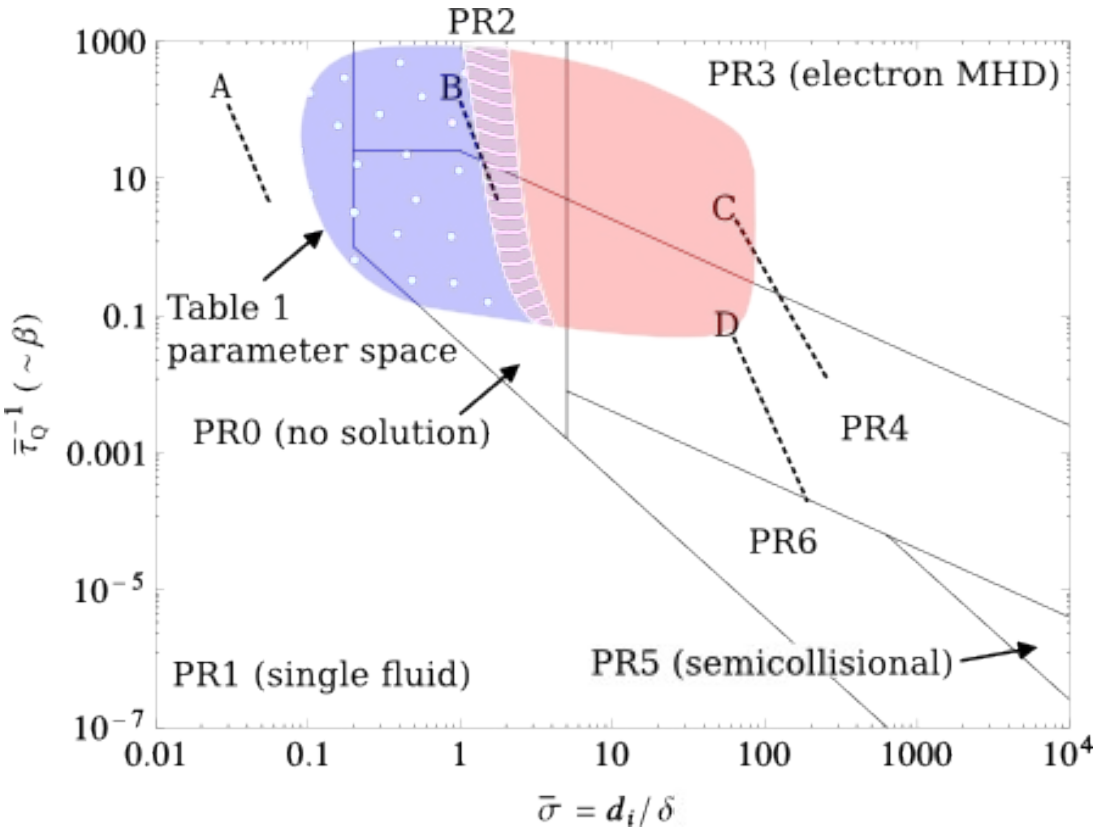

Scan A compares with the new PR2 dispersion relation in a large Λ, weakly stabilized case.

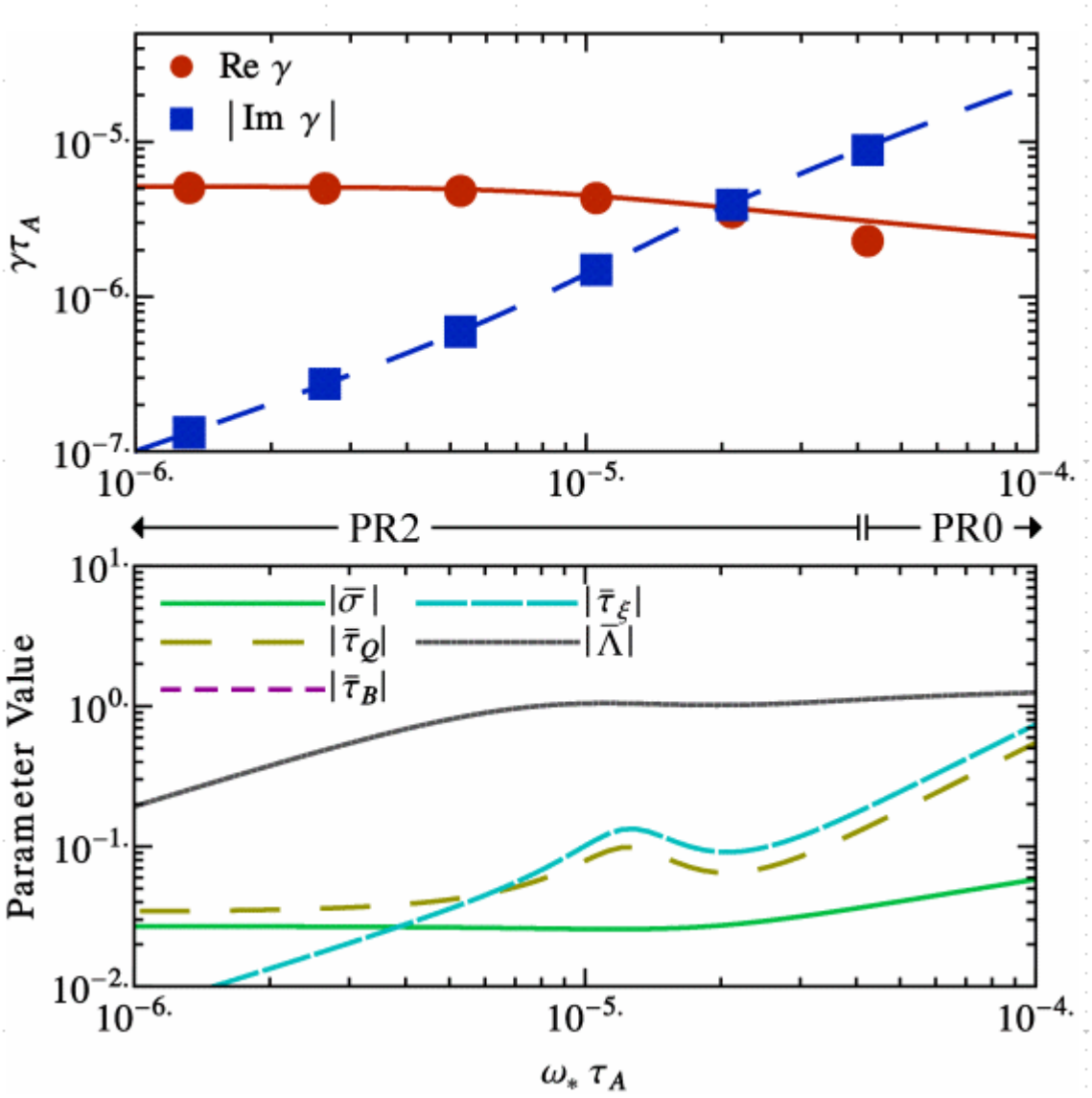

In Scan B (PR2), both the computation and analytics predict complete stabilization at large drift frequency.

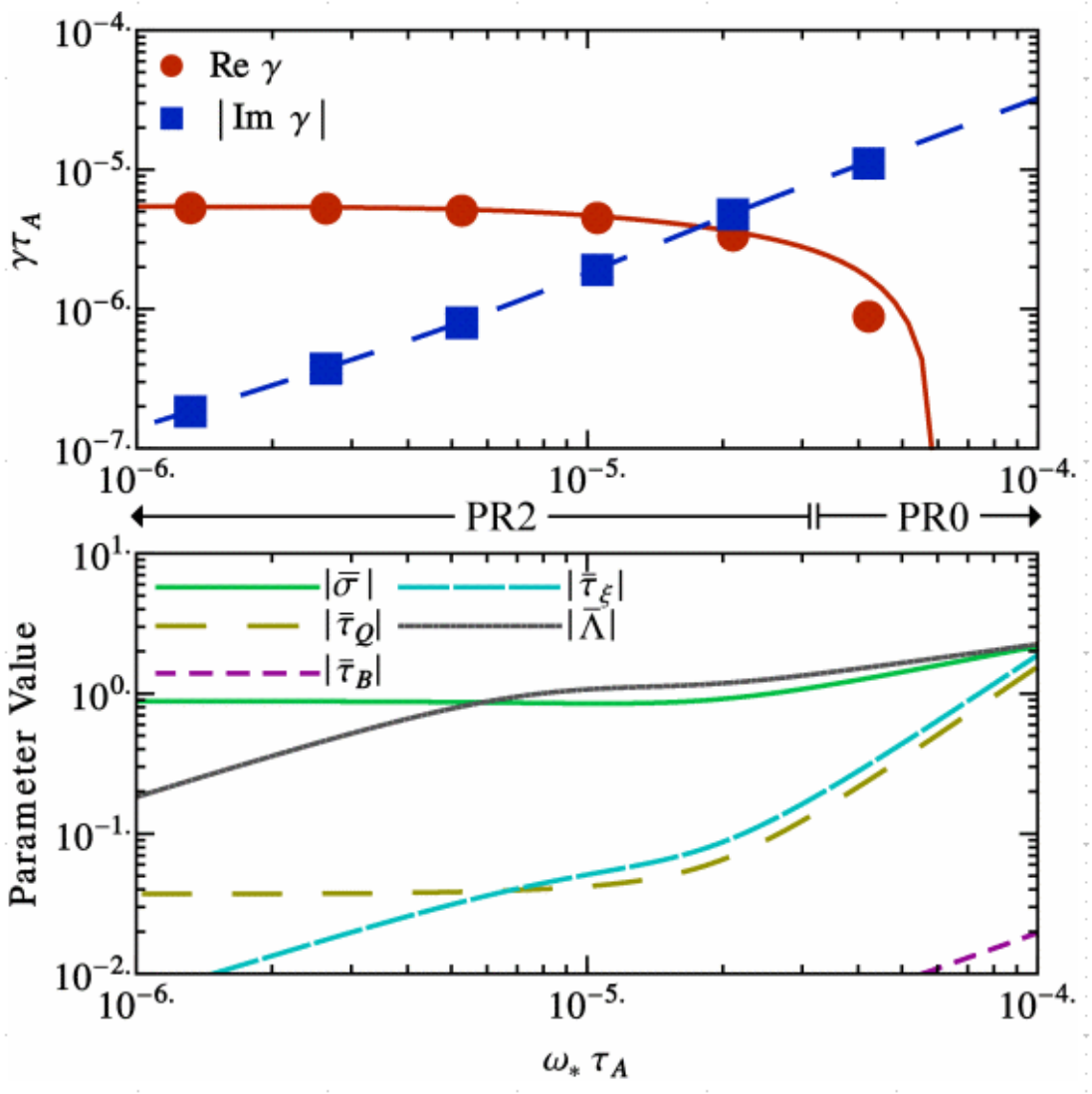

The drift-tearing response of Scan C increases the growth rate when the mode is collisionless.

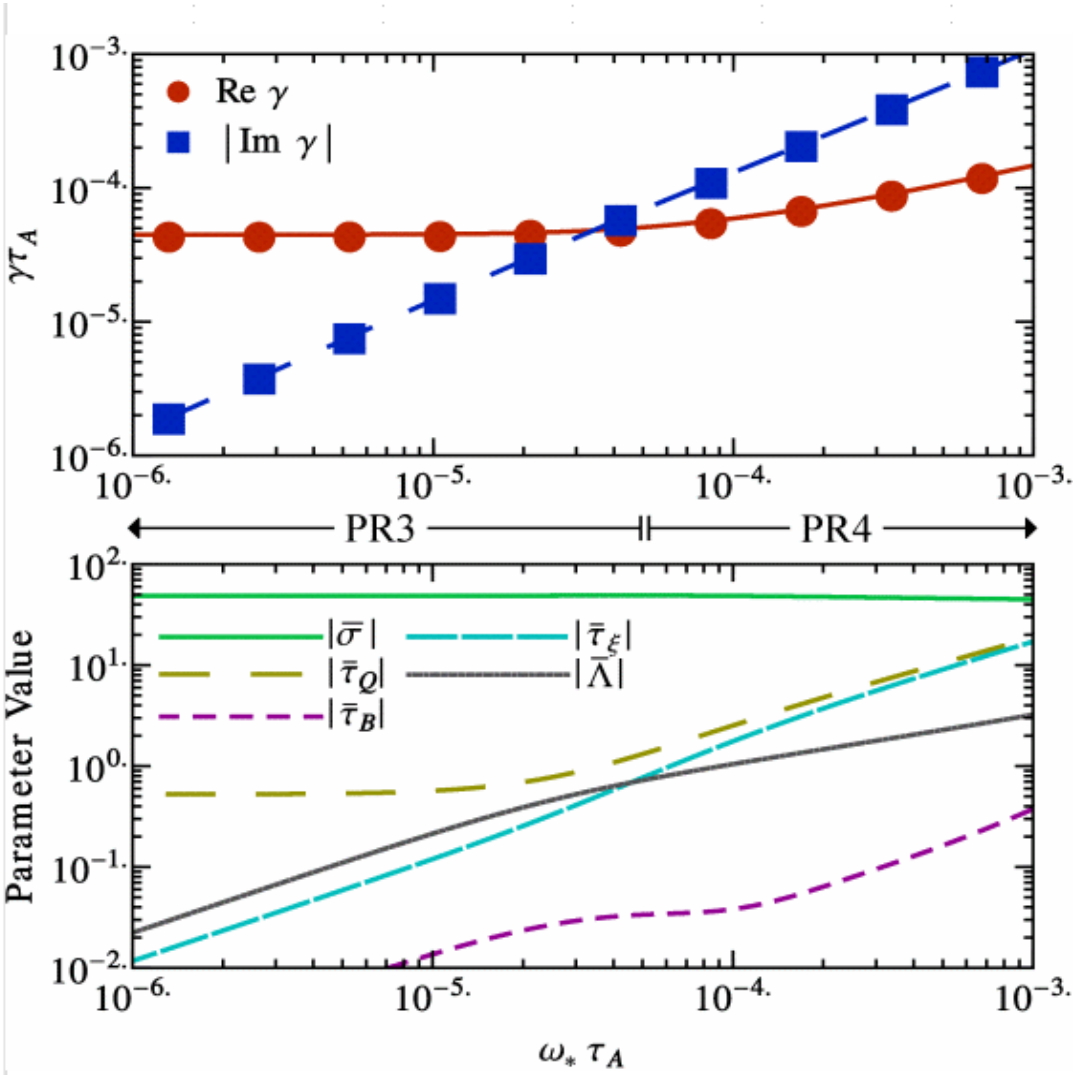

Dispersion relation:

$$\hat{\gamma}_e^2 \hat{\gamma}^{-1} = \hat{d}_e^2 \hat{d}_i \hat{k}'_{\parallel} \frac{\hat{\Delta}'^2}{2\Gamma\left(3/4\right)^4} \equiv \hat{\gamma}_c$$

Two limits:

$$\hat{\omega}_{*e} << \hat{\gamma}_c$$

$$\hat{\gamma} \simeq \hat{\gamma}_c + i\hat{\omega}_{*e}$$

$$\hat{\omega}_{*e} >> \hat{\gamma}_c$$

$$\hat{\gamma} \simeq \left(\hat{\gamma}_c + \sqrt{\hat{\omega}_{*e}\hat{\gamma}_c}\right)/2 + i\left(\hat{\omega}_{*e} + \sqrt{\hat{\omega}_{*e}\hat{\gamma}_c}/2\right)$$

This result is likely unphysical, as we needs to include electron advection and gyroviscosity to have confidence in the result from the extend-MHD model. These terms enter the system of equations on the same FLR order.

When the Scan C mode is collisional, the mode is unaffected by drift effects.

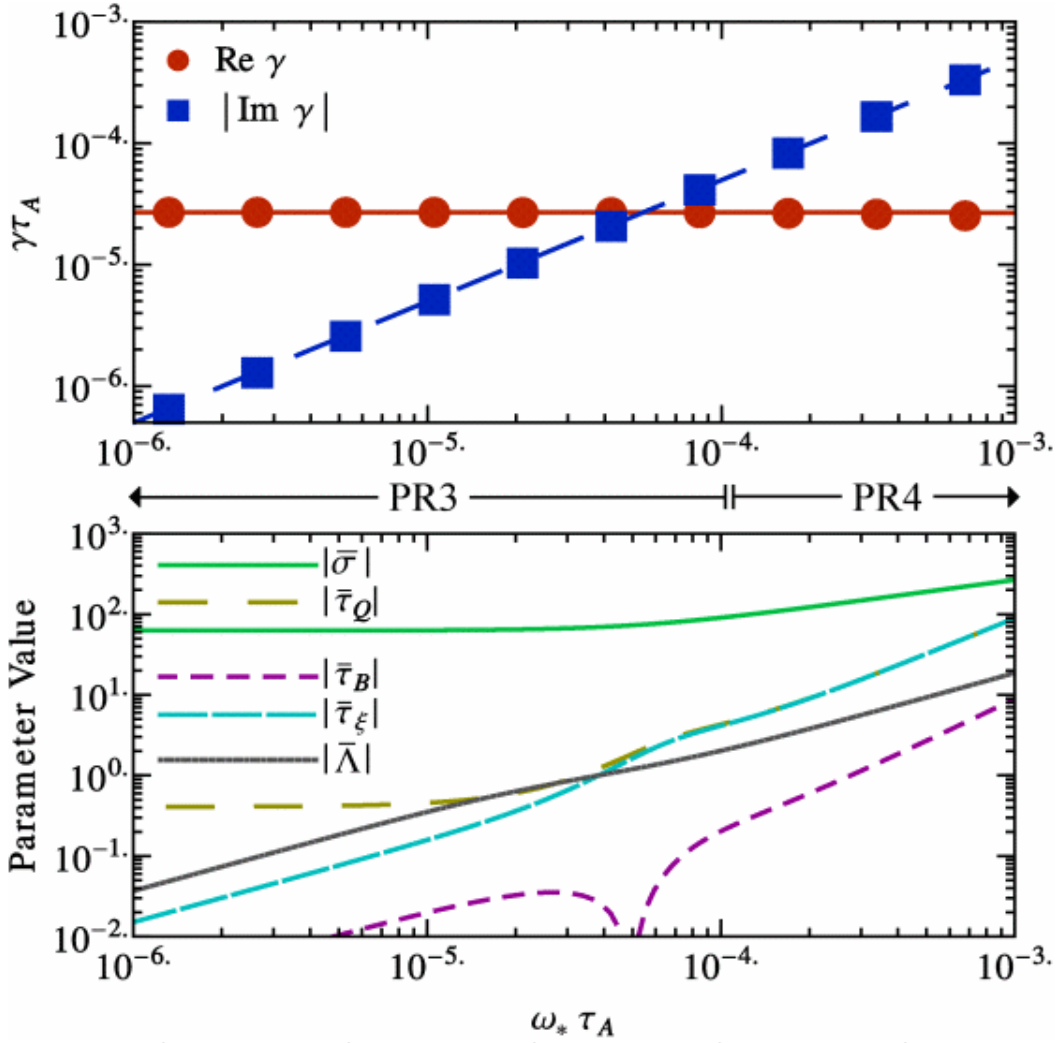

The electron mass is reduced to make the mode collisional.

The mode is dominated by the electron dynamics and simply rotates at the electron drift frequency – there is no drift stabilization.

Scan D (PR4) tests the electron temperature advection and the heat fluxes.

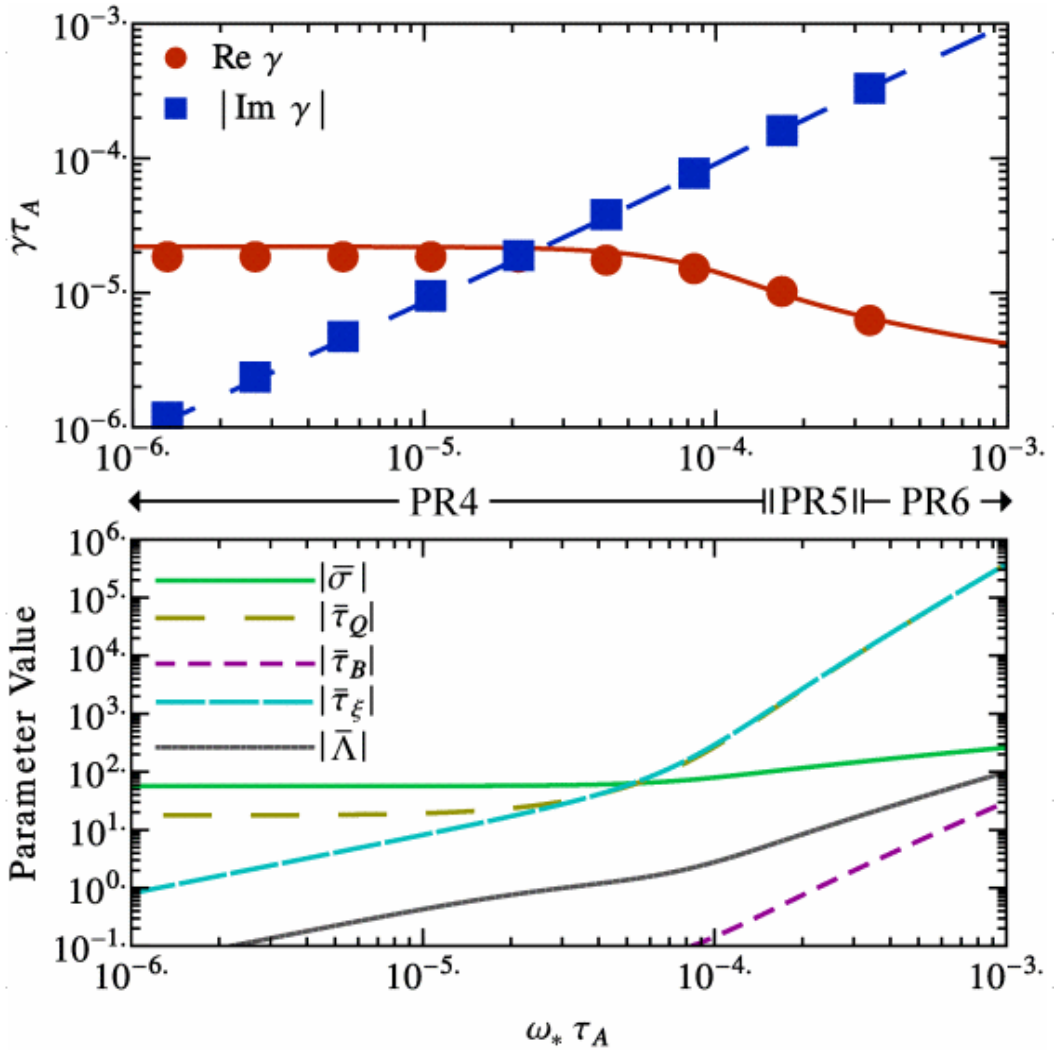

The eigenfunctions from scans A and B are largely localized to the resonant surface.

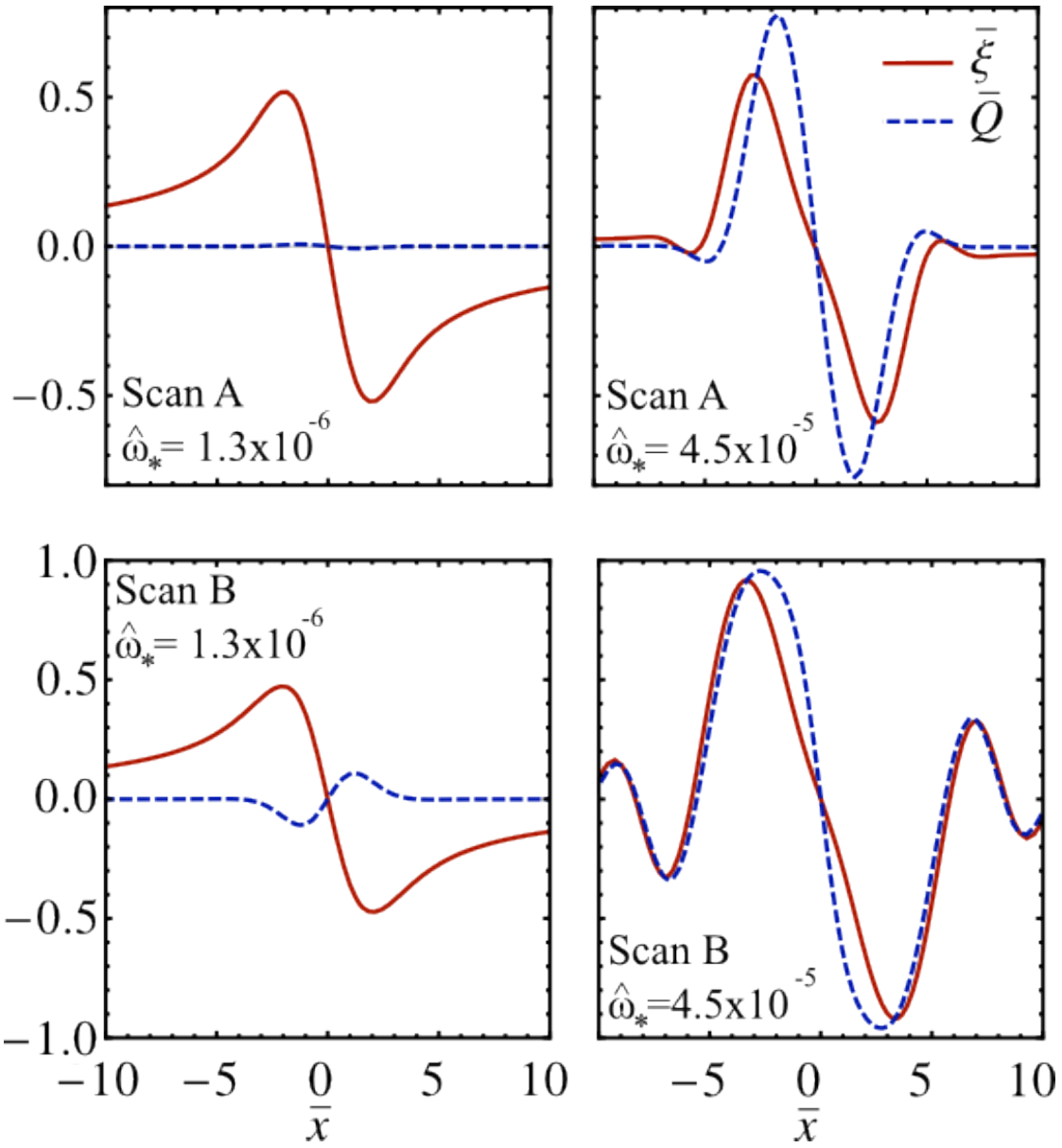

Drift effects also decouple the fluids (significant Q field, the perturbed parallel magnetic field, which is an indication of fluid decoupling).

The eigenfunction of Scans C and D are largely unmodified and global in structure, respectively.

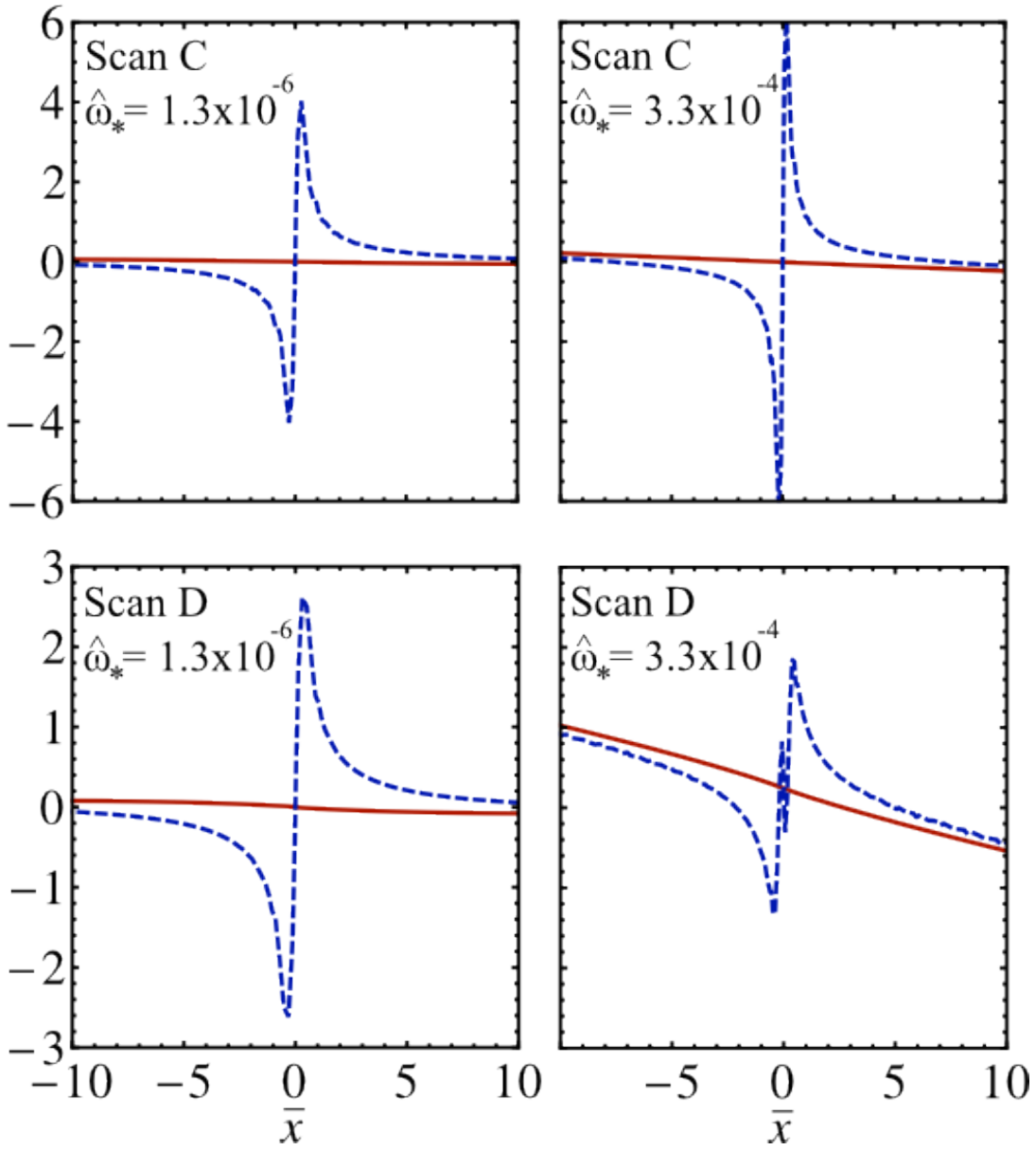

All eigenfunctions from these large ion skin depth case are dominated the contribution from Q, indicating the electron fluid dominates the layer dynamics.

The τ_B parameter is included in the PR4 analysis, however it produces an even contribution to the eigenfunction and does not affect the growth rate. This odd contribution is evident in the computational eigenfunction.

We would like to investigate the nonlinear behavior in the newly analyzed regimes.

- This is best modeled with cases where the perturbation variation is in the RZ plane.
  - Reminder: our previous cases used perturbation variation in the RPhi plane.
- Unfortunately, these cases exhibit a large wavenumber number numerical instability when the grad(pe) term is included in the induction eqn. and electron energy evolved.
  - Reminder: our previous cases used a filtering technique to restrict the computation to a single wavenumber.

We have isolated this instability to a coupling between terms with equilibrium thermodynamic gradients.

$$\frac{\partial \tilde{\mathbf{B}}}{\partial t} = \nabla \times \frac{\tilde{T}_e \nabla n}{ne}$$

$$\frac{\partial \tilde{T}_e}{\partial t} = \frac{\nabla \times \tilde{B}}{ne} \cdot \nabla T_e - T_e \frac{\nabla \times \tilde{B}}{ne} \cdot \frac{\nabla n}{n}$$

Summary

- We have characterized the drift-tearing regime and related this characterization to previous results.
- Our new analytics investigate the regime experimentally relevant for fusion discharges.
- We have used these new analytics to verify the NIMROD code.